

## Field ionization distribution curves and the local electric field

This article has been downloaded from IOPscience. Please scroll down to see the full text article.

1992 J. Phys.: Condens. Matter 4 1039

(<http://iopscience.iop.org/0953-8984/4/4/014>)

View [the table of contents for this issue](#), or go to the [journal homepage](#) for more

### Download details:

IP Address: 171.66.16.159

The article was downloaded on 12/05/2010 at 11:08

Please note that [terms and conditions apply](#).

## Field ionization distribution curves and the local electric field

Caio Mário Castro de Castilho†

Department of Chemistry, University of Cambridge, Lensfield Road, Cambridge  
CB2 1EW, UK

Received 12 November 1991

**Abstract.** Ionization probabilities of imaging gas molecules under field ion microscope conditions are calculated and compared with previous calculated and experimental results. It is shown that it is necessary to include the possibility of ionization before reaching the region close to the sample in the calculation of the curves rather than just considering the local ionization rate constant as was done previously. The presence of structure on these curves, not related to resonance states, is also shown and is interpreted as being the result of the local enhancement of the electric field close to the surface and of the cut-off of the potential barrier at points very close to the sample.

### 1. Introduction

The local electric field and its variation along atomic-size distances has been considered to be the important physical quantity in the explanation of the image contrast and resolution of the field ion microscope (FIM) (Müller and Bahadur 1956) even when disputes occurred as to whether the image formation resulted from variations of the gas concentration (Forbes 1972) or from the local ionization rate of the imaging gas molecules (Müller 1960). It now seems well established that, under normal imaging conditions, the rate-constant mechanism is dominant in determining local image contrast (Forbes 1985, de Castilho 1986).

The image in the FIM results from the ionization of gas molecules which, after ionization, are directed towards the screen (or detector) by a strong field. The position where ionization has occurred can then be inferred from the energy deficit of the molecules on arrival at the screen, compared with the energy that they would have for the full potential difference between sample and screen (Müller and Tsong 1969). Ionization distribution curves as a function of the energy deficit, or, equivalently, as a function of position, reveal several characteristics of the field ionization process. With most of the ionization occurring either close to the tip or far away from it ('free-space' field ionization—FSFI), parameters such as the width of the ionization zone or those necessary for field calibration can be determined from such curves (Müller and Tsong 1969, de Castilho and Kingham 1986).

Several years ago some structure was observed on the experimental ionization distribution curves (Jason *et al* 1965, 1966, Müller *et al* 1970), here denoted EDC

† Permanent address: Instituto de Física, UFBA, Campus Universitário da Federação, 40 210 Salvador, Bahia, Brazil.

curves. The physical interpretation for at least part of such structure has been attributed to resonant tunnelling (RT) (Jason 1967) or to surface plasmons (SP) (Lucas 1971a, b). To give support to this interpretation, Jason and Lucas have compared experimental EDC curves with calculated ones based on the variation of local ionization rate constant with position. We call these calculated curves 'IR' curves. Appelbaum and McRae (1975), using a low-energy electron diffraction calculation technique, discussed the secondary peak structure ('Jason peaks') of the EDC curves theoretically. While the resonance tunnelling process has been favoured in interpreting the Jason peaks as compared with the surface plasmon theory (Hanson and Inghram 1976), the double-peak structure within the energy-deficit distribution associated with ions produced at or very close to the critical distance has been associated with the density of surface states (Jason 1967), as a result of its surface-dependent structure (Utsumi and Smith 1974, Hanson and Inghram 1976, 1977). In these calculations the gas concentration differences are neglected; in effect, the gas concentration is assumed to be uniform.

In this paper it is pointed out that the IR curves are not themselves comparable with the ones obtained from experiment (EDC curves). This is because it is necessary to consider the possibility of the gas molecule being ionized before reaching the region close to the sample, i.e. the 'survival probability' must be taken into account. We also show that some structure on calculated distribution curves (CDC) can occur as a result of the local enhancement of the electric field and the surface proximity, even in cases where there is no structure at all present on the IR curves.

## 2. Theoretical method

We have performed one-dimensional numerical calculations based on a one-electron potential that is uniform within the metal, with height  $\Phi$  corresponding to the work function. Outside the metal the potential results from the atomic-nucleus (hydrogenic) and the external field, i.e.

$$V = -Ze^2/4\pi\epsilon_0 r - eFr \cos \phi \quad (1)$$

as adopted by Haydock and Kingham (1981). In (1)  $Ze$  is the effective nuclear charge,  $r$  is the electron's position measured from the nucleus of the gas molecule and  $\phi = \pi$ , the direction of the electric field  $F$ . This is variable along the hyperboloid-shaped tip axis, according to

$$F(z) = F_0[(1 + 2r/R_t)^{-1} + 2R^3/z^3]. \quad (2)$$

In the above equation (de Castilho and Kingham 1986)  $z$  is the distance, measured along the tip symmetry axis, from the surface of an underlying 'smooth' hyperboloid of apex radius  $R_t$  and  $F_0$  is the field at  $z = 0$ .  $R$  is the radius of a half-sphere protrusion superimposed on the apex of the hyperboloid and it is intended to simulate a local increase of the field as a result of surface structure. It is worth mentioning that the values of  $z$  to be used are greater than  $R_t$ . For typical values of  $R$  and  $R_t$  ( $\approx 2$  and  $600 \text{ \AA}$  respectively) and values of  $z$  of the order of  $20 \text{ \AA}$ , the second term within the brackets of (2) is negligible (de Castilho and Kingham 1986).

The potential barrier to be tunnelled through by the electron, when the molecule is very close to the sample surface, exhibits a sharp cut-off at the model metal surface

(Haydock and Kingham 1981). This, as will be shown below, reduces the area of the barrier and affects the local value of the ionization rate constant.

Since the electron can only tunnel to empty states of the metal, there is a minimum distance (critical distance) from which ionization can occur (Müller and Bahadur 1956) which can be approximately expressed as

$$z_c = (I - \Phi)/eF \quad (3)$$

where  $I$  is the ionization energy of the imaging gas molecule.

The polarized imaging gas molecules, under the effect of the non-uniform electric field of the FIM, drift towards the sample with a velocity at point  $z$  that can be expressed as

$$v(z) = (\alpha/m)^{1/2} F(z) \quad (4)$$

where  $\alpha$  and  $m$  are the molecular polarizability and mass, respectively. In (4) we neglect the thermal velocity and the process of accommodation of the gas molecule to the tip temperature (de Castilho and Kingham 1988).

If  $\rho(z)$  is the gas molecule ionization probability per unit distance and a molecule is assumed to exist at point  $z$ , its probability of ionization when travelling a small distance  $dz$  is given by

$$\rho(z)dz = (P_e(z)/v(z)) dz \quad (5)$$

where  $P_e(z)$  is the ionization probability per unit time, i.e. the local ionization rate constant, which we simply call the rate constant. For a gas molecule moving from a point far away towards the tip of the FIM, the probability per unit length of ionization at point  $z$  (i.e. taking into account the possibility of it having been ionized before reaching  $z$ ) is given by (de Castilho and Kingham 1986)

$$D(z) = \rho(z) \exp\left(-\int_{\infty}^z \rho(z') (-dz')\right). \quad (6)$$

Compared with the energy it would acquire if it notionally started from  $z = 0$ , a singly charged gas molecule ionized at position  $z$  reaches the screen with an energy deficit given by

$$E(z) = e \int_0^z F(z') dz' \quad (7)$$

which is the 'electrostatic energy deficit'. There are, in fact, a variety of energy-deficit parameters that, although they can be related (Forbes 1976), have different meanings. In this work, when referring to the energy deficit, we mean the value given by equation (7).

We can now convert the probability of ionization per unit length, at position  $z$ , into a probability of ionization per unit energy range, at energy deficit  $E$  corresponding to position  $z$ . Thus

$$D_e(E) = D(z)/eF(z). \quad (8)$$

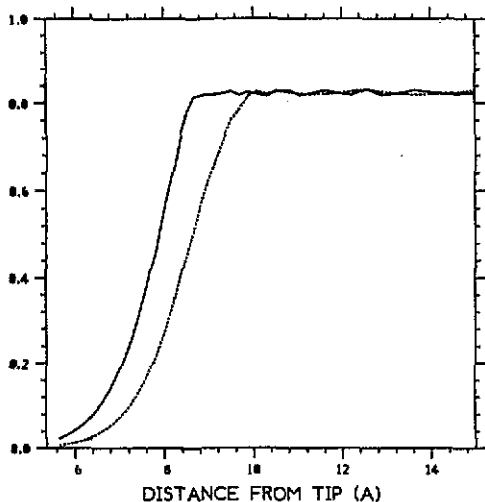


Figure 1. The ratio between the ionization rate constants, calculated using Landau's analytical approach ( $P_e(z)^{LD}$ ) and using the numerical method applied in this work ( $P_e(z)^{NUM}$ ), as a function of distance to the tip apex: —,  $R = 0.001 \text{ \AA}$ ; ·····,  $R = 1.58 \text{ \AA}$ . See equation (2).

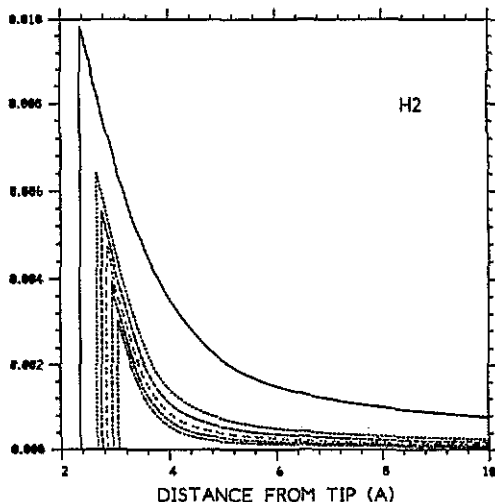


Figure 2. Ionization rate constant curves (IR) as functions of position for different values of  $F_0$  ( $R_t = 200 \text{ \AA}$  and  $R = 1.58 \text{ \AA}$ ): —,  $F_0 = 4.0 \text{ V \AA}^{-1}$ ; ·····,  $F_0 = 3.6 \text{ V \AA}^{-1}$ ; - - - -,  $F_0 = 3.5 \text{ V \AA}^{-1}$ ; ·····,  $F_0 = 3.4 \text{ V \AA}^{-1}$ ; - · - ·,  $F_0 = 3.3 \text{ V \AA}^{-1}$ ; - · · · - ·,  $F_0 = 3.2 \text{ V \AA}^{-1}$ .

The 'trajectory' of the gas molecule towards the tip is restricted to one dimension in order to keep the calculation tractable but still able to give reasonable values for experimental parameters (de Castilho and Kingham 1986).

In order to show the validity of the numerical method used here in the determination of the rate-constant,  $P_e(z)$ , we have calculated it at points along the tip symmetry axis using either the WKB numerical calculation or Landau's analytical expression (Landau and Lifshitz 1965), and then determined the ratio between this and the former. The analytical calculations, performed within the limits of validity of Landau's approach, i.e. in the region of low fields for the hydrogen atom, were done at points close to and increasingly far away from the surface. The ratio between the rate constants calculated by the two different methods,  $P_e(z)^{LD}/P_e(z)^{NUM}$ , as a function of distance from the tip surface is shown in figure 1. We have considered a smooth hyperboloidal surface for the tip surface and one with a superimposed protrusion. The sharp decreases in both curves of figure 1 result from the 'cut-off' of the potential barrier close to the surface, which is effective at larger distances when the local electric field enhancement is taken into account, i.e. when a protrusion is considered in the equation of the field (equation (2)). At points of FSFI the  $P_e(z)^{LD}/P_e(z)^{NUM}$  ratio tends towards a constant value ( $\approx 0.82$ ).

### 3. Results

We performed a one-dimensional numerical calculation of the rate constant and distribution curves (IR and CDC curves) for a  $H_2$  molecule moving along the tip axis towards the apex from a point far away. The calculations were performed for several

values of  $F_0$ , corresponding to different values of the potential difference between the tip and the screen, with the local field varying according to (2). The increase in the local field strength as a result of the surface structure, simulated in our model by the half-sphere protrusion, was varied by using different values of the half-sphere radius  $R$ .

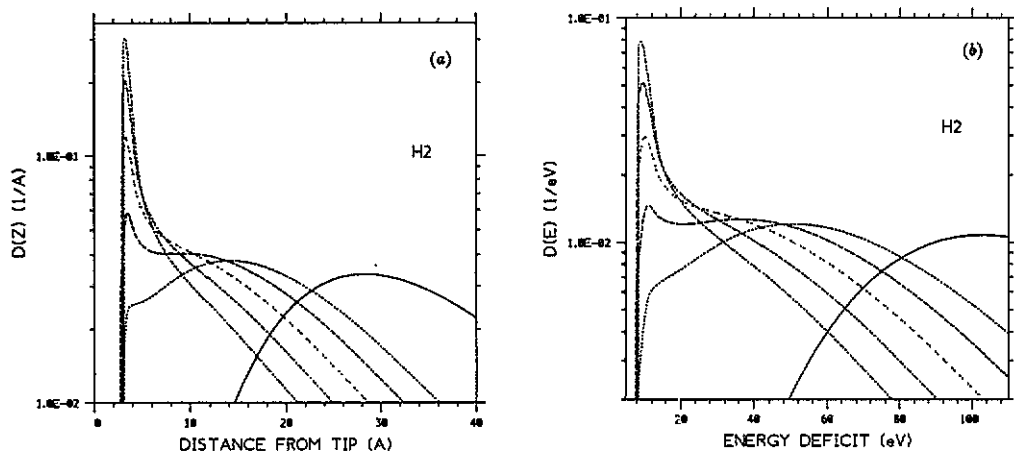


Figure 3. Calculated distribution curves (CDC) for several values of  $F_0$  as a function of: (a) position; (b) energy deficit ( $R_t = 200 \text{ \AA}$  and  $R = 1.58 \text{ \AA}$ ): —,  $F_0 = 4.0 \text{ V \AA}^{-1}$ ; ·····,  $F_0 = 3.6 \text{ V \AA}^{-1}$ ; ----,  $F_0 = 3.5 \text{ V \AA}^{-1}$ ; ·····,  $F_0 = 3.4 \text{ V \AA}^{-1}$ ; - · - ·,  $F_0 = 3.3 \text{ V \AA}^{-1}$ ; - · - ·,  $F_0 = 3.2 \text{ V \AA}^{-1}$ .

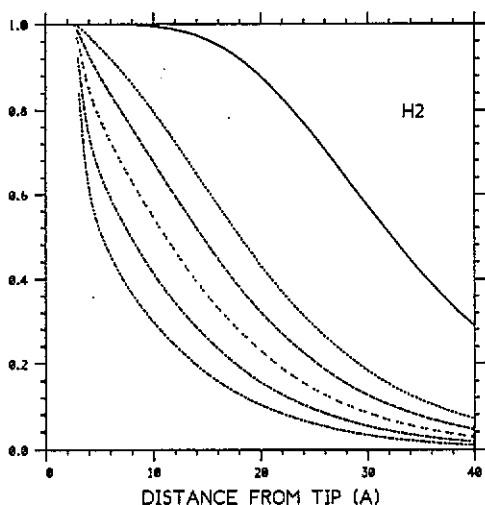


Figure 4. The total probability of a particle being ionized during its 'first approach' to the tip for different values of  $F_0$  ( $R_t = 200 \text{ \AA}$  and  $R = 1.58 \text{ \AA}$ ): —,  $F_0 = 4.0 \text{ V \AA}^{-1}$ ; ·····,  $F_0 = 3.6 \text{ V \AA}^{-1}$ ; ----,  $F_0 = 3.5 \text{ V \AA}^{-1}$ ; ·····,  $F_0 = 3.4 \text{ V \AA}^{-1}$ ; - · - ·,  $F_0 = 3.3 \text{ V \AA}^{-1}$ ; - · - ·,  $F_0 = 3.2 \text{ V \AA}^{-1}$ .

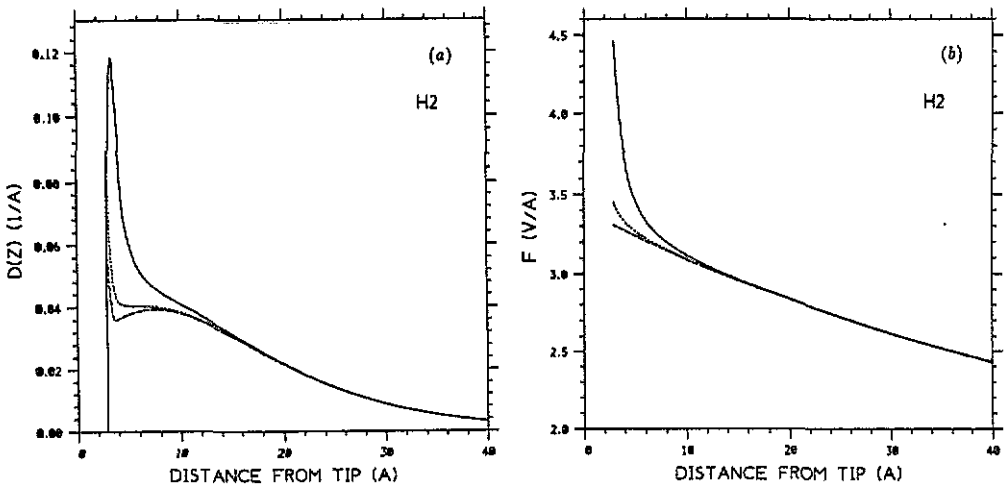


Figure 5. Variation of the calculated ionization distribution curve (a) and electric field (b) with different values for the radius of the superimposed half-sphere protrusion ( $F_0 = 3.4 \text{ V } \text{\AA}^{-1}$  and  $R_t = 200 \text{ \AA}$ ): —,  $R = 1.58 \text{ \AA}$ ; ·····,  $R = 0.79 \text{ \AA}$ ; - - -,  $R = 0.001 \text{ \AA}$ . See equation (2).

Figure 2 shows the IR curves as a function of distance from the tip for different values of  $F_0$ . Figure 3 shows the CDC curves (equations (6) and (8)) as functions of position and energy deficit for different values of  $F_0$ . Figure 4 shows the total probability ( $P(z)$ ) of the particle being ionized before reaching the tip during its 'first approach'. Figure 5 shows the effect of the local enhancement of the electric field as a result of the surface proximity, here stimulated by changing the radius of the superimposed half-sphere on the calculated distribution curves,  $\text{CDC}(z)$ .

In order to reproduce the experimental EDC curves, direct comparisons have been made with calculated IR curves (Jason 1967, Lucas 1971a, b) by assuming that 'experimental data will be approximately related to this probability through multiplication by the rate of gas supply' (Jason *et al* 1973). As can be seen from figures 2 and 3(a) the peak values of  $P_e(z)$ , numerically determined for equation (5), and of  $D(z)$ , in equation (6), do not necessarily occur in the same position. In the case of higher fields, when most of the approaching gas molecules are ionized before getting near to the sample, this causes the full curve of figure 4 to reach the value 1.0 at points about  $10 \text{ \AA}$  from the tip. In this region, the even higher field obtained due to its local enhancement, which results from the surface structure, causes an increase of the IR curve at points where  $D(z)$  has already reduced, or is very close, to zero. The IR curve is directly related to the distribution curve only for sufficiently low fields that the probability of ionization of the gas molecule away from the tip is negligible. For decreasing values of  $F_0$ , the peak of the full curve of figure 3(a) (corresponding to FSFI) moves towards the tip (de Castilho and Kingham 1986) while the total probability becomes smaller, as shown in figure 4. This corresponds to an increase in the 'survival probability' ( $1.0 - P(z)$ ).

As pointed out by Jason *et al* (1973), the gas supply to the region where the ionization occurs results from two mechanisms: (i) from surface diffusion of atoms (accommodated or partially accommodated to the tip temperature) from the shank to the tip apex; and (ii) directly from the gas phase. In the determination of  $D(z)$ ,

or alternatively  $D_e(E)$  (CDC curves), we have only considered the latter mechanism, having included the effect of polarization of the gas molecules by the external electric field.

We can see in figure 3 that for higher fields (when most of the ionization occurs away from the tip, as known from experiment) our curves  $D(z)$  and  $D_e(E)$  exhibit the correct behaviour. This result is impossible to obtain by only considering the IR curves, which do not take into account the 'survival probability'.

Figure 3(b) shows the characteristic experimental behaviour of curve 9 f of Jason (1967). For values of  $F_0$  neither too small nor high enough to give FSFI, we can see a two-peak structure that is not related to resonance states, which were not included in our calculations. This can easily be seen in figure 3. The peak closer to the tip has two causes: (i) the local enhancement of the field close to the surface—see figure 5, full and dotted lines; and (ii) the abrupt cut-off of the potential barrier as a result of the proximity of the surface. This can be seen in figure 5 (broken line) where, even for an almost negligible radius of the superimposed sphere, we have observed a sudden increase for the calculated ionization distributions. The other peak corresponds, in the case of higher fields, to the FSFI peak. The effects of these two aspects, (i) and (ii), can be seen in figure 1, for the hydrogen atom: the sharp ratio decrease resulting from the barrier 'cut-off' and the local enhancement of the electric field affecting the curves further away from the surface.

#### 4. Summary

We have shown the necessity of considering calculated ionization distributions curves,  $D(z)$  and  $D_e(E)$ , in order to make comparison with the experimental distribution measurements, as opposed to the curves previously obtained by calculation for the local ionization probability per unit time, i.e. the rate constant. In doing so, we have been able to show the possibility of double-peak formation, which results from the electric field local enhancement and from the abrupt reduction of the tunnelling barrier, both resulting from the surface proximity. Previously, multiple peaks like these were associated with surface states. Further calculations are in progress in order to obtain finer details of the ionization distribution curves close to the critical distance, aiming towards a better determination of the ionization zone width. To do this properly, an improved determination of the critical distance is necessary, instead of use of the simplified form of (3). Image potential effects can also in some way affect the results at points close to the critical distance. The validity of the numerical method used was also shown, by comparing the results for atomic hydrogen at the conditions for which Landau's analytical treatment is considered valid.

#### Acknowledgments

We are grateful to Drs R G Forbes and D R Kingham with whom we had the benefit of several discussions about the field ion microscope. We are indebted to the Department of Chemistry, University of Cambridge, particularly to Dr R M Lambert and his group, for hospitality. We are grateful to Miss D E A Gordon for improving the English of the original manuscript. This work was supported by CAPES, CNPq and UFBA (Brazil).

## References

- Appelbaum J A and McRae E G 1975 *Surf. Sci.* **47** 445-68
- de Castilho C M C 1986 *PhD Thesis* University of Cambridge
- de Castilho C M C and Kingham D R 1986 *Surf. Sci.* **173** 75-96
- 1988 *Surf. Sci.* **204** 568-86
- Forbes R G 1972 *J. Microsc.* **96** 57-61
- 1976 *Surf. Sci.* **61** 221-40
- 1985 *J. Phys. D: Appl. Phys.* **18** 973-1018
- Hanson G R and Inghram M G 1976 *Surf. Sci.* **55** 29-39
- 1977 *Surf. Sci.* **64** 305-22
- Haydock R and Kingham D R 1981 *Surf. Sci.* **103** 239-47
- Jason A J 1967 *Phys. Rev.* **156** 266-85
- Jason A J, Burns P B and Inghram M G 1965 *J. Chem. Phys.* **43** 3762-3
- Jason A J, Burns P B, Parr A C and Inghram M G 1966 *J. Chem. Phys.* **44** 4351-2
- Jason A J, Parr A C and Inghram M G 1973 *Phys. Rev. B* **7** 2883-6
- Landau L D and Lifshitz E M 1965 *Quantum Mechanics* (Oxford: Pergamon) section 77
- Lucas A A 1971a *Phys. Rev. Lett.* **26** 813-6
- 1971b *Phys. Rev. B* **4** 2939-49
- Müller E W 1960 *Adv. Electron. Electron Phys.* **13** 83-179
- Müller E W and Bahadur K 1956 *Phys. Rev.* **102** 624-31
- Müller E W, Krishnaswamy S V and McLane S B 1970 *Surf. Sci.* **23** 112-29
- Müller E W and Tsong T T 1969 *Field Ion Microscopy: Principles and Applications* (Amsterdam: Elsevier)
- Utsumi T and Smith N V 1974 *Phys. Rev. Lett.* **33** 1294-7